Volume 5, No. 5, September 2011   ISSN: 1750-5836

INTERNATIONAL JOURNAL OF

Greenhouse Gas Control

ELSEVIER

ieaghg
Published in association
with the IEA Greenhouse
Gas R&D Programme

Available online at www.sciencedirect.com
SciVerse ScienceDirect

Performance of amine-multilayered solid sorbents for CO_2 removal: Effect of fabrication variables

Bingbing Jiang [a,b,c], Vincent Kish [c], Daniel J. Fauth [b], McMahan L. Gray [b],
Henry W. Pennline [b], Bingyun Li [a,b,c,d,*]

[a] National Energy Technology Laboratory, U.S. Department of Energy, Morgantown, WV 26505, United States
[b] National Energy Technology Laboratory, U.S. Department of Energy, Pittsburgh, PA 15236, United States
[c] School of Medicine, West Virginia University, Morgantown, WV 26506, United States
[d] WVNano Initiative, Morgantown, WV 26506, United States

ARTICLE INFO

ABSTRACT

The emission of fossil fuel carbon dioxide (CO_2) to the atmosphere is implicated as the predominant cause of global climate change; therefore, advanced CO_2 capture technologies are of the utmost importance. In this study, innovative amine-multilayered sorbents were fabricated using layer-by-layer (LbL) nanoassembly technology via alternate deposition of a CO_2-adsorbing amine polymer (e.g. polyethylenimine or PEI) and an oppositely-charged polymer (e.g. polystyrene sulfonate or PSS). We found that the developed sorbents could be used for CO_2 capture and that LbL nanoassembly allows us to engineer their CO_2 capture performance through the fabrication variables (e.g. deposition polymers, deposition media, and number of bilayers). PEI/PSS was found to be the best polymer combination for developing sorbents with relatively high CO_2 capture capacity. The amine-multilayered solid sorbents possessed fine microstructures and may have similar polymer deposition within and on the surface of solid sorbents. These amine-multilayered sorbents had much faster CO_2 desorption rates compared to sorbents prepared using the current PEI-impregnation approach. Such fast CO_2 desorption could make sorbents a good option for CO_2 removal from power plants and even the atmosphere.

1. Introduction

Carbon dioxide (CO_2) is considered to be one of the major greenhouse gases directly influencing global climate change and human health, as more than 30 billion tons of anthropogenic CO_2 is annually added to the atmosphere, and its emission is continuously increasing. The United States is the 10th largest emitter of CO_2 emissions per capita as of 2004 (Raupach et al., 2007). Due to the continuous rise of CO_2 in the atmosphere, extensive interest has been shown in developing carbon sequestration technologies, which may trap and store large quantities of CO_2 from concentrated sources such as power plants (Figueroa et al., 2008). Capture is a key step in the overall carbon sequestration technologies. Various approaches have been reported for capturing and separating CO_2 such as aqueous amine sorption (Hook, 1997; Meisen and Shuai, 1997; Rao and Rubin, 2002; Aaron and Tsouris, 2005; Song et al., 2006; Lee et al., 2007), membrane separation (FalkPedersen and Dannstrom, 1997; Luebke et al., 2006), and cryogenic separation (White et al., 2003). Aqueous amine absorption has already been applied on the commercial scale for CO_2 separation from power plant flue gas (Aaron and Tsouris, 2005). However, aqueous amine absorption has high operating costs due to the heat of sorption plus the sensible and latent heating of the solution. Extensive water is required to prevent equipment corrosion and avoid airflow problems, which consequently results in high energy requirements for regeneration. Meanwhile, loss of amine components due to degradation and evaporation at moderate temperatures is another problem for aqueous amine absorption (Ma'mun et al., 2005; Mandal and Bandyopadhyay, 2005, 2006).

To avoid these problems, solid sorbents have been developed, e.g. amine immobilized materials including silica (Tsuda et al., 1992; Gray et al., 2005; Knowles et al., 2005; Hicks and Jones, 2006; Harlick and Sayari, 2007; Hicks et al., 2008; Drese et al., 2009), fly ash (Gray et al., 2004), molecular sieves (Xu et al., 2002, 2003, 2005; Ma et al., 2009; Wang et al., 2009), activated carbons (Siriwardane et al., 2001; Shigemoto et al., 2005; Alesi et al., 2010), and polymer supports (Satyapal et al., 2001; Filburn et al., 2005; Schladt et al., 2007). These amine solid sorbents offer several

* Corresponding author at: Biomaterials, Bioengineering and Nanotechnology Laboratory, Department of Orthopaedics, School of Medicine, West Virginia University, Morgantown, WV 26506-9196, United States. Tel.: +1 304 293 1075; fax: +1 304 293 7070.
E-mail address: bli@hsc.wvu.edu (B. Li).
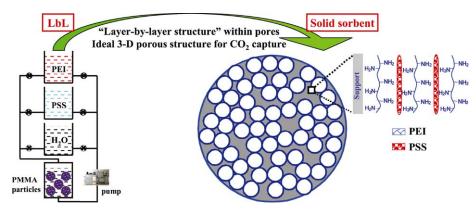*URL:* http://www.hsc.wvu.edu/som/ortho/nanomedica-group/ (B. Li).

Fig. 1. Preparation of amine-multilayered solid sorbents using LbL nanoassembly.

advantages including their capability to be used at low pressure for CO_2 recovery, low capital cost, and low regeneration energy compared to aqueous amine solvents (Siriwardane et al., 2001; Xu et al., 2002; Khatri et al., 2006; Ma et al., 2009). Amines can be physically absorbed or chemically bonded in porous sorbents, and CO_2 capture is mainly based on the interaction between primary and secondary amines with gaseous CO_2 molecules (Hook, 1997; Gray et al., 2005). Although macromolecular amines may have better regeneration capacity and thermal stability, amines with low molecular weights have been primarily studied to date (Gray et al., 2004, 2005, 2008; Hicks et al., 2008).

We recently piloted the development of solid sorbents using layer-by-layer (LbL) nanoassembly (Li et al., 2011), which is a unique technique for manufacture of composite nanofilms. LbL nanoassembly has been extensively studied to develop a variety of highly-selective and multifunctional multilayer films based on the alternate deposition of oppositely-charged polyelectrolytes on a substrate surface including metal, silicone, glass, and inorganic/organic colloid (Decher, 1997). The attractive feature of this technology is its ability to construct multilayers at the nanometer scale and to integrate polymers of interest within a hierarchical porous architecture (Decher, 1997). Our previous studies in the biomedical fields have shown that the LbL fabrication variables (e.g. polymer components, deposition medium, number of layers) have played a major role in tuning the properties of polyelectrolyte multilayer films (Li and Haynie, 2004; Li et al., 2005, 2009; Zhong et al., 2006; Zhao and Li, 2008; Jiang and Li, 2009; Jiang et al., 2010). In this study, we investigated, for the first time, the effect of LbL fabrication variables on the properties, including CO_2 capture capacity, of amine-multilayered solid sorbents, and identified the best polymer combinations for nano-layered sorbents.

2. Methodology

2.1. Chemicals

PEI (MW = 10,000), PSS (MW = 70,000), poly(allylamine hydrochloride) (PAH, MW = 56,000), poly(acrylic acid) (PAA, MW = 15,000), methanol, ethanol (EtOH), dimethyl sulfoxide (DMSO), Rhodamine B (RhoB), and fluorescein isothiocyanate (FITC) were purchased from Sigma Aldrich Co. (St. Louis, MO). PEI, PSS, PAH, and PAA were each dissolved in deionized water at a concentration of 10 mg/ml. PEI in methanol and PSS in DMSO/EtOH (30/70% v/v) were also prepared at a concentration of 10 mg/ml and 1 mg/ml, respectively. In addition, PEI of 400 and 800 mg/ml were prepared in methanol. Polymethylmethacrylate (PMMA) microparticles were purchased from Supelco Co. (Bellefonte, PA) with the following manufacturer specifications: effective particle size 0.5 mm; pore volume 1.2 ml/g; specific surface area 470 m^2/g;
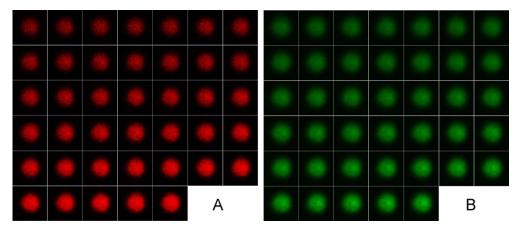
and density 0.29 g/ml. PMMA sheets were obtained from United States Plastic Corp. (Lima, OH). N_2 and CO_2 of high purity were used for thermogravimetric analysis (TGA). Fluorescent labeled polymers, which could be visualized under fluorescent microscopy, were used as indicators of polymer deposition and multilayer formation. RhoB-PEI and FITC-PSS were synthesized as reported (Volodkin et al., 2004). After stirring for 2 h at room temperature, the solutions were dialyzed against deionized water for two days and stored for further use.

2.2. Preparation of PEI-multilayered PMMA sorbents

LbL nanoassembly was used to prepare PEI-multilayered sorbents. A vacuum pump was applied to remove air and to run the solutions through the interior pores of sorbent supports (i.e. PMMA particles). Amine-multilayered sorbents were prepared at room temperature. PMMA microparticles were packed in a custom-made deposition chamber. Vacuum was applied first for 30 min then the following procedures were carried out under 380 torr to prepare PEI-multilayered sorbents in aqueous media (Fig. 1): (i) A positively-charged polymer (e.g. PEI or PAH) solution was run through PMMA microparticles for 15 min, then the microparticles were rinsed with deionized water twice for 15 min. (ii) A negatively-charged polymer (e.g. PSS or PAA) solution was run through the PMMA supports followed by two similar water rinses. The completion of these procedures, i.e. deposition of one layer of a positively-charged polymer and a second layer of a negatively-charged polymer followed by rinses, were designated as one deposition cycle or one bilayer. By repeating these deposition cycles, amine-multilayered sorbents were fabricated and were dried under vacuum at 80 °C overnight until further use. Similarly, PEI-multilayered sorbents were also prepared in organic solvents when PEI in methanol and PSS in DMSO/EtOH were used as deposition materials and methanol was used as the rinsing medium. The flow rates for all media were approximately 150 ml/min.

2.3. Preparation of PEI-impregnated PMMA sorbents

PEI-impregnated PMMA sorbents were prepared using a well studied wet impregnation method (Gray et al., 2005, 2009; Khatri et al., 2006; Hicks et al., 2008). In brief, PEI was dissolved in methanol at a concentration of 400 or 800 mg/ml under a rotary evaporator (RV 10 basic plus D, Wilmington, NC) using a stirring rate of 100 rpm. After 15 min, PMMA microparticles were added. The suspension was continuously stirred for about 30 min under a manual water pump (450 torr vacuum) and subsequently dried at 60 °C for 2 h.

Fig. 2. Z-stack images visualized under CLSM with excitation/emission wavelengths of (A) 543/580 nm and (B) 488/525 nm of Rhodamine B-labeled PEI (RhoB-PEI) and fluorescein isothiocyanate-labeled PSS (FITC-PSS) deposited (PEI/PSS)$_{10}$ multilayered PMMA beads. The red and green indicate the distributions of PEI and PSS, respectively. Interval thickness of each slice is 0.9 μm, Z-stack size is 113 μm. (For interpretation of the references to color in this figure legend, the reader is referred to the web version of the article.)

2.4. Characterization

PMMA sorbents were examined using confocal laser scanning microscopy or CLSM (Zeiss 510 Meta Confocal Microscope, Thornwood, NY), scanning electron microscopy (SEM, Hitachi S-4700, Tokyo, Japan), ellipsometry (M-2000, J.A. Woollam., Lincoln, NE), and TGA (Perkin Elmer, Waltham, MA). PMMA sorbents were cut into halves. Images of the cross-sections of RhoB-PEI and FITC-PSS deposited PMMA sorbents were also taken in a z-stack mode to visualize the distribution of the two polymers. In addition, PMMA microparticles, cut into halves or intact, were glued onto stainless steel supports and sputtered with gold. SEM and energy dispersive X-ray (EDX) analysis were conducted on the surfaces of whole (intact) and on the cross-sections of broken PMMA sorbents. The value of N/C ratio was averaged from five randomly selected samples. To estimate the thickness of each bilayer, polymer multilayers were formed on planar PMMA sheets under similar deposition conditions as they were deposited in PMMA microparticles and ellipsometry measurements were conducted.

The CO$_2$ capture performance of amine-multilayered PMMA sorbents was determined using TGA (Gray et al., 2009) and compared to one of the most commonly studied solid sorbents, i.e. PEI-impregnated PMMA sorbents (Gray et al., 2005, 2009; Khatri et al., 2006; Hicks et al., 2008). Approximately 50 mg of PMMA-based sorbent was loaded in the TGA microbalance quartz sample cell. The sample was heated at 105 °C in N$_2$ atmosphere for about 60 min, and the temperature was then lowered to 40 °C. The adsorption cycle was carried out at 40 °C under pure dry CO$_2$ until no obvious weight gain was observed. A desorption cycle was subsequently performed at 40 °C using a pressure-swing approach by means of introducing pure N$_2$ into the sample cell. All gas flow rates were set at 200 ml/min. The weight change in milligrams (mg) of the PMMA particles was recorded and the weight change in percentage was defined as the ratio of the amount of the gas evolved, adsorbed or desorbed over the total amount of CO$_2$ adsorbed. Adsorption capacity in mol CO$_2$/(kg sorbent) was calculated from the weight change of the samples during the adsorption and desorption cycles. In addition, adsorption capacity in mol CO$_2$/(kg PEI) was estimated, assuming equal amounts of positively- and negatively-charged polymers were deposited in the PMMA sorbents.

3. Results

Polyethylenimine/polystyrene sulfonate (PEI/PSS) multilayered solid sorbents were prepared using LbL nanoassembly (Fig. 1). The

distribution of PEI and PSS within PMMA particles was examined using CLSM. Both PEI and PSS were confirmed to be deposited uniformly throughout the (PEI/PSS)$_{10}$ multilayered PMMA particles (Fig. 2). Note that the subscript refers to the number of bilayers or deposition cycles. More polymers (i.e. PEI and PSS) were deposited with an increasing number of PEI/PSS bilayers (Fig. 3). Moreover, the nitrogen/carbon (N/C) ratio increased with increasing PEI/PSS bilayers and the N/C ratios on the PMMA particle surfaces and within the multilayered PMMA particles were found to be approximately the same in the (PEI/PSS)$_{10}$ multilayered PMMA samples; however, a substantially higher (68% more) N/C ratio was detected on surfaces of the PEI-impregnated PMMA particles compared to those of their interior surfaces (Fig. 4). In addition, the PEI/PSS multilayered PMMA sorbents had very fine porous structures while the PEI-impregnated PMMA sorbents were much less porous (Fig. 5).

The fabrication variables (e.g. deposition cycle, polymer component, and deposition medium) of the LbL nanoassembly process influenced the CO$_2$ capture capacity of the developed solid sorbents (Table 1). The (PEI/PSS)$_{10}$ PMMA, prepared in water media almost doubled the capacity, in mol CO$_2$/(kg sorbent), of (PEI/PSS)$_5$ PMMA, and had slightly higher capacity compared to (PEI/PSS)$_{10}$ PMMA prepared in organic solvents. Replacing PSS with a weak polyelectrolyte (i.e. PAA) or replacing PEI with PAH led to a substantial decrease in CO$_2$ capture capacity. For instance, the capacity decreased from 1.7 mol CO$_2$/(kg sorbent) of (PEI/PSS)$_{10}$ PMMA to a little adsorption, i.e. 0.1 mol CO$_2$/(kg sorbent), of (PEI/PAA)$_{10}$ PMMA. Moreover, the PEI/PSS multilayered sorbents had high
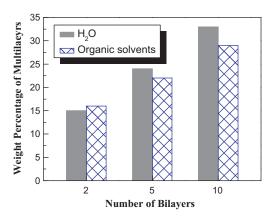

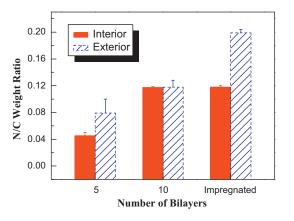**Fig. 3.** Weight percentage of PEI/PSS multilayers in PMMA sorbents.

Fig. 4. N/C weight ratio of PEI/PSS multilayered and PEI-impregnated PMMA sorbents.

Table 1

CO_2 capture capacity of amine-multilayered PMMA solid sorbents under pure CO_2 atmosphere.

Sample	CO_2 capture capacity		
	mol CO_2/ (kg sorbent)	mol CO_2/ (kg PEI)[b]	mol CO_2/ mol N[b,c]
$(PEI/PSS)_5$ PMMA	0.8	12.8	0.56
$(PEI/PSS)_{10}$ PMMA	1.7	17.4	0.77
$(PEI/PSS)_{10}$ PMMA[a]	1.4	16.8	0.74
$(PEI/PAA)_{10}$ PMMA	0.1	1.8	0.08
$(PAH/PSS)_{10}$ PMMA	0.5	9.6	0.55

[a] Prepared in organic solvents.

[b] Calculated from mass increase before and after polymer deposition, assuming equal amounts of positively- and negatively-charged polymers were deposited.

[c] Amine efficiency.

amine efficiency, i.e. the CO_2/N ratio, up to 0.77 mol CO_2/mol N for the $(PEI/PSS)_{10}$ PMMA sorbents. In addition, the deposition medium may have also influenced the thickness of PEI/PSS multilayers, as the thickness (~10 nm/bilayer) of PEI/PSS deposited in organic solvents was slightly higher than that (~8 nm/bilayer) of PEI/PSS deposited in water media (Fig. 6).

Compared to PEI-impregnated PMMA sorbents, PEI/PSS multilayered solid sorbents showed substantially faster CO_2 desorption rates during sorbent regeneration and relatively faster CO_2 adsorption rates during adsorption cycles (Fig. 7A). At the same capacity, e.g. 0.8 mol CO_2/(kg sorbent), the desorption of CO_2 from PEI/PSS multilayered sorbents was much faster (3 min vs. 36 min for 50% desorption) than from PEI-impregnated PMMA sorbents (Table 2). It may take hours at a minimum to desorb CO_2 from PEI-impregnated PMMA sorbents. It was found that within 30 min, more CO_2 was desorbed from PEI/PSS multilayered sorbents than
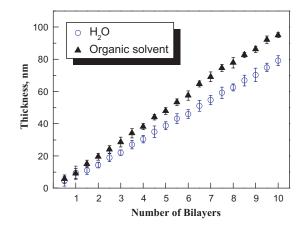

Fig. 6. Multilayer thickness vs. number of PEI/PSS bilayers, which were assembled on planar surfaces of PMMA sheets in an aqueous or organic medium.

Table 2

CO_2 desorption from PEI/PSS multilayered and PEI-impregnated PMMA sorbents under pure CO_2 atmosphere.

Sample	CO_2 capture capacity, mol CO_2/ (kg sorbent)	Time for 50% desorption, min[a]	30-min desorption, mol CO_2/ (kg sorbent)[a]
$(PEI/PSS)_5$ PMMA	0.8	3	0.75
$(PEI/PSS)_{10}$ PMMA	1.7	16	1.02
PEI impregnated	0.8	36	0.65
PMMA	3.4	300	0.37

[a] Data obtained from Fig. 7.

from PEI-impregnated PMMA sorbents (Table 2). Increasing PEI/PSS bilayers from 5 to 10 significantly improved the desorption of CO_2 at a given time period (e.g. 30 min). Interestingly, two- or three-fold CO_2 was desorbed within 30 min from $(PEI/PSS)_5$ and $(PEI/PSS)_{10}$ PMMA sorbents than from PEI-impregnated PMMA sorbents which had a several-fold higher capacity of 3.4 mol CO_2/(kg sorbent) (Fig. 7B).

4. Discussion

Carbon dioxide is one of the major greenhouse gases directly influencing global climate change because of its effect on the earth's ozone layer; its emission may have contributed to urban smog, acid rain, and health problems (Song, 2006; EPA, 2011). In this study, innovative amine-multilayered solid sorbents were developed using a recently evolved nanotechnology, named LbL nanoassembly (Decher, 1997). PEI (a CO_2-adsorbing polymer) and PSS, positively- and negatively-charged polymers, respectively, were finely deposited in the porous structure of PMMA
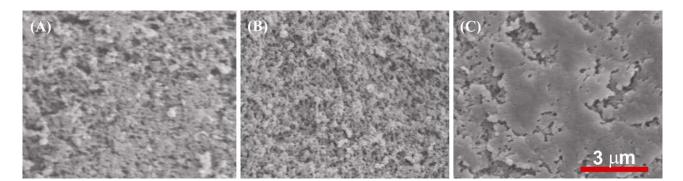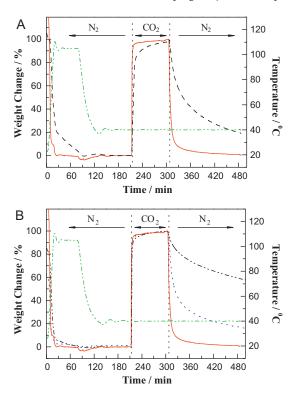

Fig. 5. Interior porous structure of PEI/PSS multilayered and PEI-impregnated sorbents: (A) $(PEI/PSS)_5$ PMMA, (B) $(PEI/PSS)_{10}$ PMMA, and (C) PEI-impregnated PMMA. The pictures share the same scale bar.

Fig. 7. CO_2 adsorption capacity of PEI/PSS multilayered and PEI-impregnated sorbents under pure CO_2 atmosphere. (A) Samples of the same CO_2 capture capacity, i.e. 0.8 mol CO_2/(kg sorbent). ▬▬▬ (PEI/PSS)$_5$ PMMA, ▬▬ PEI-impregnated PMMA (PEI concentration of 800 mg/ml was used at a 1:2 ratio of PEI to PMMA). (B) Samples of different CO_2 capture capacity, 0.8, 1.7 and 3.4 mol CO_2/(kg sorbent). ▬▬▬ (PEI/PSS)$_5$ PMMA of 0.8 mol CO_2/(kg sorbent), ●●●●●● (PEI/PSS)$_{10}$ PMMA of 1.7 mol CO_2/(kg sorbent), ▮▮▮▮▮ PEI-impregnated PMMA of 3.4 mol CO_2/(kg sorbent) (PEI concentration of 400 mg/ml was used at a 1:1 ratio of PEI to PMMA). Temperature (dashed green lines). (For interpretation of the references to color in this figure legend, the reader is referred to the web version of the article.)

microparticles (Figs. 2 and 5(A and B)). It was found that the fabrication variables significantly influenced the properties of the developed multilayered solid sorbents. Substantially higher CO_2 capture capacity was obtained for (PEI/PSS)$_{10}$ PMMA sorbents than (PEI/PAA)$_{10}$ and (PAH/PSS)$_{10}$ PMMA sorbents. This may indicate that the alternate layers of a strong polyelectrolyte (i.e. PSS) compared to a weak one (i.e. PAA) could substantially enhance the accessibility and deposition of the CO_2-adsorbing polymer (i.e. PEI) thereby leading to higher CO_2 capture capacity (Table 1). The number of PEI/PSS bilayers as well as the deposition medium influenced the PEI/PSS multilayer structure and thereby the CO_2 capture capacity. With an increasing number of PEI/PSS bilayers, more polymers (PEI and PSS) were deposited into the PMMA particles (Fig. 3) and, as a result, the thickness of the PEI/PSS bilayer (Fig. 6) and the N/C ratio increased (Fig. 4). Consequently, the CO_2 capture capacity was almost doubled when the PEI/PSS bilayers were doubled from 5 to 10 (Table 1). In addition, the improved distribution or deposition of polymers inside and outside the PMMA microparticles (Fig. 4) may have improved the accessibility of the CO_2-adsorbing polymer (i.e. PEI). Further tuning of the multilayer structure (e.g. uniformity of the layers) thereby sorbent properties may be achieved via salt (e.g. NaCl) and polymer concentrations, use of solvent, and application of vacuum or pressure.

Under dry conditions, the maximum amine efficiency of an amine adsorbent is 0.5 mol CO_2/mol N, however, higher amine efficiency was also reported (Harlick and Sayari, 2007; Serna-Guerrero et al., 2008; Choi et al., 2009). As reviewed by Choi et al. (2009), and Harlick and his colleagues (Harlick and Sayari, 2007; Serna-Guerrero et al., 2008), the amine efficiency of amine

adsorbents reported in the literature under dry conditions varied within a wide range from 0.025 to 0.89, and it was suggested that physisorption of CO_2 besides chemisorption by amines contributed to the total capacities (Serna-Guerrero et al., 2008; Choi et al., 2009). In this study, the amine efficiency of PEI/PSS multilayered sorbents varied from 0.56 to 0.77 mol CO_2/mol N, and similarly, physisorption of CO_2 contributed partially to the CO_2 capture capacity.

One major motivation for developing solid sorbents is that they may require substantially less energy for regeneration than current aqueous amine CO_2 scrubbing (Hoffman et al., 2008; Li et al., 2010). One challenge of most solid sorbents still lies in the slow CO_2 desorption rate; it may take hours or days for the desorption process where diffusion resistance is high (Satyapal et al., 2001). PEI/PSS multilayered solid sorbents were found to be advantageous in CO_2 adsorption and desorption, since PEI/PSS multilayered PMMA sorbents showed very fine distribution of PEI within the PMMA particles (Fig. 5) and fast CO_2 adsorption and desorption rates (Fig. 7). Compared to one of the most well studied solid sorbents (i.e. PEI-impregnated PMMA sorbents) (Gray et al., 2005, 2009; Khatri et al., 2006; Hicks et al., 2008), PEI/PSS multilayered solid sorbents had a much faster CO_2 desorption rate (Table 2). Within a reasonably short time period (i.e. 30 min), twice or three times the CO_2 was desorbed from amine-multilayered solid sorbents compared to the PEI-impregnated sorbents, even though the latter had much higher CO_2 capture capacity. The enhancement of amine-multilayered solid sorbents in CO_2 desorption rate possibly was due to the unique nano-layered and fine microstructure, which may facilitate CO_2 transport, of the PEI/PSS multilayered sorbents versus the densely-packed microstructure of the PEI-impregnated sorbents (Fig. 5). Multilayer coatings prepared by LbL nanoassembly have shown hierarchical nanofilm architectures with nano-scale pores (Mendelsohn et al., 2000), which could be especially suitable for substance (e.g. CO_2) transport. Another possible reason for the fast desorption rate is that the heat of adsorption over the LbL assembled PEI could be much lower than that of the PEI-impregnated sorbents. The PEI amine sites in the multilayered sorbents are partially neutralized by PSS thereby these sites may bind acidic CO_2 more weakly than uncomplexed PEI. In addition, the uniform distribution or deposition of polymers inside and outside the PMMA microparticles (Fig. 4) may have also facilitated CO_2 transport during its adsorption and desorption processes. Therefore, PEI/PSS multilayered PMMA sorbents had fast adsorption and desorption rates (Fig. 7 and Table 2). Note that pressure swing was applied in this study and practical regeneration systems will likely include thermal swing which will provide additional heat for regeneration. As a result, faster desorption rate is expected with combination of pressure swing and thermal swing.

5. Conclusions

LbL nanoassembly was applied to fabricate amine-multilayered solid sorbents for CO_2 removal. The LbL fabrication variables including polymer components and deposition cycles were used to optimize the CO_2 capture properties of amine-multilayered solid sorbents. Compared to (PEI/PAA)$_{10}$ and (PAH/PSS)$_{10}$, (PEI/PSS)$_{10}$ multilayered sorbents showed the highest CO_2 capture capacity. More polymers were deposited with increasing deposition cycles. Also, the deposition medium was found to influence the multilayer thickness. Most importantly, the developed amine-multilayered solid sorbents had fine microstructures and fast CO_2 desorption rates. Further experiments in simulated flue-gas stream (e.g. 10%CO_2/H_2O/90%He), multiple cycles, and isosteric heat of adsorption of CO_2 will be carried out in future studies.

Conflict of interest

None.

Acknowledgements

References

Aaron, D., Tsouris, C., 2005 Sep. Sci. Tech. 40, 321–348.

Alesi Jr., W.R., Gray, M., Kitchin, J.R., 2010. ChemSusChem 3, 948–956.

Choi, S., Drese, J.H., Jones, C.W., 2009. ChemSusChem 2 (9), 796–854.

Decher, G., 1997. Science 277 (5330), 1232–1237.

Drese, J.H., Choi, S., Lively, R.P., Koros, W.J., Fauth, D.J., Gray, M.L., Jones, C.W., 2009. Adv. Funct. Mater. 19 (23), 3821–3832.

EPA, 2011. Greenhouse Gases Threaten Public Health and the Environment/Science Overwhelmingly Shows Greenhouse Gas Concentrations at Unprecedented Levels Due to Human Activity. http://yosemite.epa.gov/opa/admpress.nsf/0/08D11A451131BCA585257685005BF252 (accessed 23.02.11.).

FalkPedersen, O., Dannstrom, H., 1997. Energy Convers. Manage. 38, 81–86.

Figueroa, J.D., Fout, T., Plasynski, S., McIlvried, H., Srivastava, R.D., 2008. Int. J. Greenhouse Gas Control 2 (1), 9–20.

Filburn, T., Helble, J.J., Weiss, R.A., 2005. Ind. Eng. Chem. Res. 44, 1542–1546.

Gray, M.L., Champagne, K.J., Fauth, D., Baltrus, J.P., Pennline, H., 2008. Int. J. Greenhouse Gas Control 2, 3–8.

Gray, M.L., Hoffman, J.S., Hreha, D.C., Fauth, D.J., Hedges, S.W., Champagne, K.J., Pennline, H.W., 2009. Energy Fuels 23, 4840–4844.

Gray, M.L., Soong, Y., Champagne, K.L., Baltrus, J.R.W., Stevens, J., Toochinda, P., Chuang, S.S.C., 2004. Purif. Technol. 35 (September), 31–36.

Gray, M.L., Soong, Y., Champagne, K.J., Pennline, H., Baltrus, J.P., Stevens, R.W., Khatri, R., Chuang, S.S.C., Filburn, T., 2005. Fuel Process. Technol. 86 (14–15), 1449–1455.

Harlick, P.J.E., Sayari, A., 2007. Ind. Eng. Chem. Res. 46, 446–458.

Hicks, J.C., Drese, J.H., Fauth, D.J., Gray, M.L., Qi, G.G., Jones, C.W., 2008. J. Am. Chem. Soc. 130 (10), 2902–2903.

Hicks, J.C., Jones, C.W., 2006. Langmuir 22, 2676–2681.

Hoffman, J., Richards, G.A., Pennline, H.W., Fischer, D., Keller, G., 2008. Proceedings of the 33rd International Technical Conference on Coal Utilization and Fuel Systems, Clearwater FL, 1–5 June, 2008, Paper 120. Coal Technology Association, Gaithersburg MD, ISBN 978-0r-r932066-336.

Hook, R.J., 1997. Ind. Eng. Chem. Res. 36, 1779–1790.

Jiang, B., DeFusco, E., Li, B., 2010. Biomacromolecules 11, 3630–3637.

Jiang, B., Li, B., 2009. Int. J. Nanomed. 4, 37–53.

Khatri, R.A., Chuang, S.S.C., Soong, Y., Gray, M., 2006. Energy Fuels 20, 1514–1520.

Knowles, G.P., Graham, J.V., Delaney, S.W., Chaffee, A.L., 2005. Fuel Process. Technol. 86, 1435–1448.

Lee, S., Song, H.J., Maken, S., Park, J.W., 2007. Ind. Eng. Chem. Res. 46, 1578–1583.

Li, B., Haynie, D.T., 2004. Biomacromolecules 5 (5), 1667–1670.

Li, B., Haynie, D.T., Palath, N., Janisch, D., 2005. J. Nanosci. Nanotechnol. 12 (5), 2042–2049.

Li, B., Jiang, B., Boyce, B., Lindsey, B., 2009. Biomaterials 30, 2552–2558.

Li, B., Jiang, B., Fauth, D.J., Gray, M.L., Pennline, H.W., Richards, G.A., 2011. Chem. Commun. 47, 1719–1721.

Li, W., Choi, S., Drese, J.H., Hornbostel, M., Krishnan, G., Eisenberger, P.M., Jones, C.W., 2010. ChemSusChem 3, 899–903.

Luebke, D., Myers, C., Pennline, H., 2006. Energy Fuels 20, 1906–1913.

Ma, X.L., Wang, X.X., Song, C.S., 2009. J. Am. Chem. Soc. 131 (16), 5777–5783.

Ma'mun, S., Nilsen, R., Svendsen, H.F., Juliussen, O., 2005. J. Chem. Eng. Data 50, 630–634.

Mandal, B.P., Bandyopadhyay, S.S., 2005. Chem. Eng. Sci. 60, 6438–6451.

Mandal, B.P., Bandyopadhyay, S.S., 2006. Chem. Eng. Sci. 61, 5440–5447.

Meisen, A., Shuai, X., 1997. Energy Convers. Manage. 38, 37–42.

Mendelsohn, J.D., Barrett, C.J., Chan, V.V., Pal, A.J., Mayes, A.M., Rubner, M.F., 2000. Langmuir 16, 5017–5023.

Rao, A.B., Rubin, E.S., 2002. Environ. Sci. Technol. 36, 4467–4475.

Raupach, M.R., Marland, G., Ciais, P., Le Quéré, C., Canadell, J.G., Klepper, G., Field, C.B., 2007. Proc. Nat. Acad. Sci. U.S.A. 104 (24), 10288–10293.

Satyapal, S., Filburn, T., Trela, J., Strange, J., 2001. Energy Fuels 15 (2), 250–255.

Schladt, M., Fiburn, T.P., Helble, J.J., 2007. Ind. Eng. Chem. Res. 46, 1590–1597.

Serna-Guerrero, R., Da'na, E., Sayari, A., 2008. Ind. Eng. Chem. Res. 47, 9406–9412.

Shigemoto, N., Yanagihara, T., Sugiyama, S., Hayashi, H., 2005. J. Chem. Eng. Jpn. 38, 711–717.

Siriwardane, R.V., Shen, M.S., Fisher, E.P., Poston, J.A., 2001. Energy Fuels 15, 279–284.

Song, C.S., 2006. Catal. Today 115 (1–4), 2–32.

Song, H.J., Lee, S., Maken, S., Park, J.J., Park, J.W., 2006. Fluid Phase Equilib. 246, 1–5.

Tsuda, T., Fujiwara, T., Takteani, Y., Saeguas, T., 1992. Chem. Lett. 21, 2161–2164.

Volodkin, D.V., Petrov, A.I., Prevot, M., Sukhorukov, G.B., 2004. Langmuir 20 (8), 3398–3406.

Wang, X.X., Schwartz, V., Clark, J.C., Ma, X.L., Overbury, S.H., Xu, X.C., Song, C.S., 2009. J. Phys. Chem. C 113, 7260–7268.

White, C.M., Strazisar, B.R., Granite, E.J., Hoffman, J.S., Pennline, H.W., 2003. J. Air Waste Manage. Assoc. 53 (6), 645–715.

Xu, X.C., Song, C.S., Andresen, J.M., Miller, B.G., Scaroni, A.W., 2002. Energy Fuels 16, 1463–1469.

Xu, X.C., Song, C.S., Andresen, J.M., Miller, B.G., Scaroni, A.W., 2003. Microporous Mesoporous Mater. 62, 29–45.

Xu, X.C., Song, C.S., Miller, B.G., Scaroni, A.W., 2005. Ind. Eng. Chem. Res. 44, 8113–8119.

Zhao, Q., Li, B., 2008. Nanomedicine: NBM 4, 302–310.

Zhong, Y., Li, B., Haynie, D.T., 2006. Biotechnol. Prog. 22 (1), 126–132.